ORIGINAL RESEARCH

Expression Profiles and Bioinformatic Analysis of Circular RNAs in Db/Db Mice with Cardiac Fibrosis

Lingling Yuan[1], Ting Wang[1], Jinsheng Duan[2], Jing Zhou[1], Na Li [1], Guizhi Li[1], Hong Zhou [1]

[1]Department of Endocrinology, the Second Hospital of Hebei Medical University, Shijiazhuang, Hebei, 050004, People's Republic of China;
[2]Department of Cardiology, the Second Hospital of Hebei Medical University, Shijiazhuang, Hebei, 050004, People's Republic of China

Correspondence: Hong Zhou, Department of Endocrinology, the Second Hospital of Hebei Medical University, Shijiazhuang, Hebei, People's Republic of China, Tel +86-15130119625, Email zhoubs2013@hebmu.edu.cn; zhoubs2013@163.com

Introduction: Cardiac fibrosis is one of the important causes of heart failure and death in diabetic cardiomyopathy (DCM) patients. Circular RNAs (circRNAs) are covalently closed RNA molecules in eukaryotes and have high stability. Their role in myocardial fibrosis with diabetic cardiomyopathy (DCM) remain to be fully elucidated. This study aimed to understand the expression profiles of circRNAs in myocardial fibrosis with DCM, exploring the possible biomarkers and therapeutic targets for DCM.

Methods: At 21 weeks of age, db/db mice established the type 2 DCM model measured by echocardiography, and the cardiac tissue was extracted for Hematoxylin–eosin, Masson's trichrome staining, and transmission electron microscopy. Subsequently, the expression profile of circRNAs in myocardial fibrosis of db/db mice was constructed using microarray hybridization and verified by real-time quantitative polymerase chain reaction. A circRNA–microRNA–messenger RNA coexpression network was constructed, Gene Ontology and Kyoto Encyclopedia of Genes and Genomes pathway enrichment analysis were done.

Results: Compared with normal control mice, db/db mice had 77 upregulated circRNAs and 135 downregulated circRNAs in their chromosomes (fold change ≥1.5, P ≤ 0.05). Moreover, the enrichment analysis of circRNA host genes showed that these differentially expressed circRNAs were mainly involved in mitogen-activated protein kinase signaling pathways. CircPHF20L1, circCLASP1, and circSLC8A1 were the key circRNAs. Moreover, circCLASP1/miR-182-5p/Wnt7a, circSLC8A1/miR-29b-1-5p/Col12a1, and most especially circPHF20L1/miR-29a-3p/Col6a2 might be three novel axes in the development of myocardial fibrosis in DCM.

Conclusion: The findings will provide some novel circRNAs and molecular pathways for the prevention or clinical treatment of DCM through intervention with specific circRNAs.

Keywords: Circular RNAs, expression profile, diabetic cardiomyopathy, cardiac fibrosis, bioinformatic analysis

Introduction

Circular RNAs (circRNAs) are covalently closed RNA molecules in eukaryotes that have high stability; compared with linear RNAs, they are more resistant to exonucleases.[1] CircRNAs mainly act as microRNA (miRNA) sponges, protecting target messenger RNAs from miRNA-dependent degradation; therefore, the target RNA is more actively translated and bound by ribosomes.[2]

In patients with diabetes, diabetic cardiomyopathy (DCM) is a specific cardiovascular complication that first manifests as diastolic dysfunction and eventually progresses to refractory heart failure. Myocardial fibrosis is a critical pathological feature of DCM.[3] However, the mechanism involved in the development of myocardial fibrosis in DCM remains unclear.

CircRNAs have been reported to play an important role in myocardial fibrosis in DCM.[4–6] A recent study found that diabetes-induced circulation-associated circRNA (DICAR) was downregulated in diabetic mouse hearts and was associated with a negative fibrosis index in DICAR-deficient mice.[7] Tang et al determined that circ_000203 was upregulated in the myocardium from mouse models of type 2 diabetes mellitus (T2DM) and increased the expression of colla2, colla3, and α-smooth muscle actin in cardiac fibroblasts (CFs), thereby exacerbating myocardial fibrosis.[4] In another study, circRNA_010567 was increased in the myocardium from T2DM mice, and knockdown of this circRNA

remarkably suppressed myocardial fibrosis via the miR-141/TGF-b1 pathway in angiotensin II (AngII)-induced CFs.[5] CircHIPK3 was found to be upregulated in mouse DCM models induced by streptozotocin, and knockdown of this circRNA could ameliorate myocardial fibrosis and cardiac function in vivo and decrease CF proliferation induced by Ang II via the miR-29b-3p/Col1a1-Col3a1 pathway in vitro.[6] Unfortunately, this study did not perform echocardiography on db/db mice and used Ang II to induce fibroblast fibrosis instead of high glucose (HG), which may not fully reflect the pathogenesis of myocardial fibrosis in HG conditions. Recently, three studies have analyzed the competitive endogenous RNA (ceRNA) network in cardiac fibrosis/DCM/cardiac hypertrophy.[8–10] To date, no study has investigated ceRNAs for myocardial fibrosis induced by T2DM in vivo.

Hence, the present study aimed to understand the expression profiles and the role of circRNAs and ceRNAs in myocardial fibrosis in DCM using bioinformatic analysis. DCM models were first confirmed through measurement of cardiac function and pathologic changes, and then systematic circRNAs in the myocardium were screened.

Materials and Methods
Animal Study
Eight-week-old male diabetic db/db mice (N = 8) weighing 39g to 41g and eight-week-old male control C57BL/6 mice (N = 8) weighing 19g to 21g were obtained from Nanjing Junke Bioengineering Co., Nanjing, China. At 8 weeks of age, all db/db mice exhibited fasting blood glucose levels $\geq$ 11.1mmol/L. The mice were housed at an ambient temperature of 22°C with a 12-h light/dark cycle and maintained on a normal chow diet. All experimental procedures were approved by the Animal Experimentation Ethics Committee of the Second Hospital of Hebei Medical University (NO. 2022-AE132), and the experimental methods were performed in accordance with the approved guidelines for the Care and Use of Laboratory Animals by the National Institutes of Health. At the age of 21 weeks, the body weight, heart weight/tibia length ratio, and fasting blood-glucose levels of mice were measured and was mentioned in Figure 1 the flow chart of animal experiment. Fasting blood-glucose levels were measured using the automatic biochemical instrument at the Second Hospital of Hebei Medical University. Serum fasting
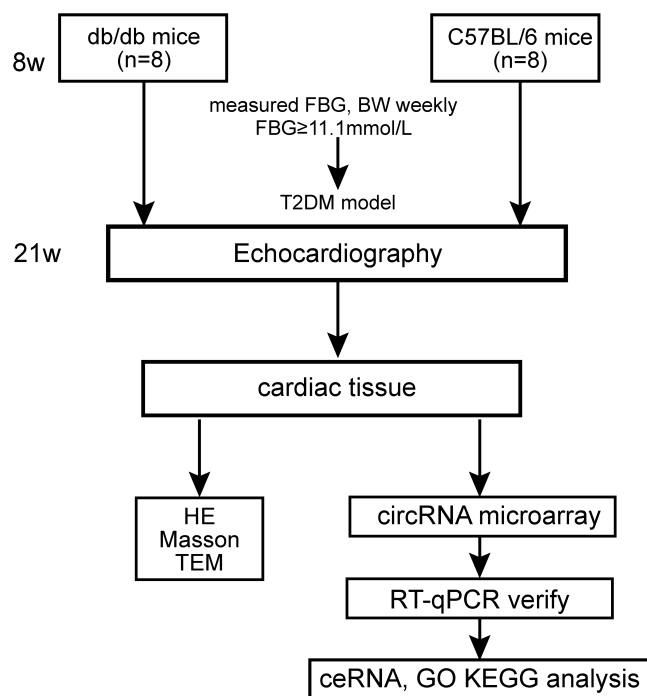

Figure 1 Flow chart of animal experiment.
Abbreviations: BW, body weight; CeRNA, competitive endogenous RNA; DCM, diabetic cardiomyopathy; FBG, fasting blood glucose; GO, Gene Ontology; HE, hematoxylin–eosin; KEGG, Kyoto Encyclopedia of Genes and Genomes; RT-qPCR, Real-time polymerase chain reaction; T2DM, Type 2 diabetes mellitus; TEM, transmission electron microscopy.

insulin levels were determined using an ELISA kit (Senberga, Nanjing, China) following the manufacturer's instructions. The purpose of this two different model was to establish the diabetic cardiomyopathy model and normal control model. We replicated the animal model of DCM using method in a literature.[11] Three mice were randomly selected from each group of mice for detection using the random number method in echocardiography, hematoxylin–eosin (H & E) and masson's trichrome staining, transmission electron microscopy and circRNA microarray analysis part.

Echocardiography

At 21 weeks of age, the cardiac function of mice was evaluated by transthoracic echocardiography with an 11-MHz linear transducer coupled to a high-resolution ultrasound system (Vivid E95, GE Healthcare, USA). Isoflurane was used as an inhaled anesthetic in mice with an induction dose of 2% and a maintenance dose of 1%. During the whole process, the mice were placed on a warming pad, and their heart rates were maintained at 400–500 beats/min. Left ventricular (LV) function was assessed by the following parameters: LV ejection fraction (EF), LV fractional shortening (FS), LV internal diameter in diastole (LVIDd), and LV internal dimension systole (LVIDs), which were calculated using computer algorithms. Subsequently, the mitral peak flow velocities at early diastole (E) and atrial contraction (A) were detected using the pulsed Doppler technique. Tissue Doppler imaging was obtained from the lateral mitral valve annulus, and the early diastolic mitral annular velocity (e′) was measured. The E/A and E/e′ ratios were calculated to reflect LV diastolic function. Measurements were averaged for three consecutive cardiac cycles by an experienced technician.[12] None of the mice experienced spontaneous mortality during the course of the experiment.

H & E and Masson's Trichrome Staining

The mice were euthanized by CO_2 inhalation combined with cervical dislocation, the flow rate was set at 50% of the chamber, and the death verification of the mice was no response when the front paw of mice was clamped with hemostatic forceps. Cardiac tissue was taken and fixed in 4% paraformaldehyde. Thereafter, it was dehydrated, embedded in paraffin, and sectioned at a thickness of 5 μm. The sections were stained with H & E staining and Masson's trichrome. Masson's trichrome staining was used to assess the extent of fibrosis in cardiac tissue.

Sample Preparation for Transmission Electron Microscopy

Cardiac tissues were acutely isolated from db/db mice and control mice. Subsequently, they were immediately placed in 2.5% glutaraldehyde and kept at 4°C. The samples were dehydrated, embedded, and cut into ultrathin sections with thicknesses of 50–100 nm. The ultrastructure of cardiac tissue was observed by transmission electron microscopy (HT7800, Hitachi, Tokyo, Japan).

CircRNA Microarray and Data Analysis

Cardiac tissue samples were randomly collected from db/db (n = 3) and control (n = 3) mice at the age of 21 weeks. Total RNA was extracted from the cardiac apex of mice using TRIzol reagent (Invitrogen, Carlsbad, CA) and quantified using the Nanodrop ND-1000 Spectrophotometer (Thermo Scientific, Wilmington, DE). The microarray analysis of circRNAs was performed by Kangcheng Biotech (Shanghai, China). Total RNA was digested with RNase R (Epicenter, Wisconsin, USA) to remove linear RNAs. The enriched circRNAs were amplified and transcribed into fluorescent complementary RNA (cRNA) using a random priming method (Arraystar Super RNA Labeling Kit, Arraystar). The labeled cRNAs were hybridized onto the Arraystar Mouse circRNA Array V2 (8x15K, Arraystar). After the slides were washed, the arrays were scanned with the Agilent Scanner G2505C. Agilent's Feature Extraction software (version 11.0.1.1) was used to analyze the acquired array images.[4] The R software limma package was used to perform quantile normalization and subsequent data processing. Differentially expressed circRNAs with statistical significance between two groups were identified through volcano plot filtering. Differentially expressed circRNAs between two groups were identified through fold change filtering. CircRNAs with fold changes ≥1.5 and $P \leq 0.05$ were considered as significantly differentially expressed. The distinguishable circRNA expression patterns among samples were determined using hierarchical clustering.

Real-time Quantitative Polymerase Chain Reaction (RT-qPCR)

Total RNA was extracted from tissues using TRIzol reagent (Invitrogen, Carlsbad, CA) in accordance with the manufacturer's protocols. Total RNA was digested with RNase R (Epicenter, Inc.) to remove linear RNAs. Then, RNA (1 μg) was reverse-transcribed into complementary DNA using Superscript™ III Reverse Transcriptase (Invitrogen, Carlsbad, CA). Subsequently, PCR was performed on the QuantStudio 5 Real-time PCR System (Applied Biosystems) using 2× PCR master mix (Arraystar) in accordance with the manufacturer's instructions. The thermo-cycling conditions were used in RT-qPCR: 95°C for 10min; 40 cycles of 95°C for 10 sec, and 60°C for 60 sec; and a final extension at 99°C for 10min. All the primers in this study are shown in Table 1. Primers are designed by Sangon Biotech. CircRNA primers are divergent primers. They were designed using Primer 3 Plus based on circRNA gene sequence in Data S1. The housekeeping gene ACTB was used as an internal control.[13] The relative expression (fold change) was analyzed using the $2-\Delta\Delta CT$ method.[14]

Construction of the ceRNA Network

Target RNAs/miRNAs were predicted using a homemade miRNA target prediction software based on TargetScan (http://www.targetscan.org/vert_71/) and miRanda (http://www.microrna.org/microrna/ home.do) to find the potential targets of miRNAs. A ceRNA network were constructed by merging the common targeted miRNAs. Three conditions must exist for the ceRNA network to occur:[15] first, the relative concentration of ceRNAs and their miRNAs is clearly important; second, the effectiveness of a ceRNA would depend on the number of miRNAs that it can "sponge"; third, not all miRNA recognition elements on ceRNAs are equal. Therefore, only these ceRNA-pair relations that passed some filtering measures were accepted.

Gene Ontology (GO) and Kyoto Encyclopedia of Genes and Genomes (KEGG) Pathway Enrichment Analysis

The GO project provides a controlled vocabulary to describe gene and gene product attributes in any organism (http://www.geneontology.org). The ontology covers three domains: biological process, cellular component, and molecular function. Fisher's exact test in the topGO package (Bioconductor) was used to determine whether there was more overlap between the differentially expressed list and the GO annotation list than would be expected by

Table 1 The Sequences of Primers of Verified circRNAs

Target	Primer Sequences (5'-3')
circRNA_28667	Forward, 5' GTCGCTATTACCCTGCCAAGA3', reverse, 5' GTAGTCCAGTGCCTCCAAACG3';
circRNA_32303	Forward, 5' AGTGAAGATAGGGCTGGGGA3', reverse, 5' AGGCCTGGCATGAAGAACTC 3';
circRNA_20674	Forward, 5' AACCTGGCTGCTATCAAGATGC3', reverse, 5' TTCACAGAACCAGGGATTCGTC 3';
circRNA_25425	Forward, 5' CTTTAGAGTCAGAGTATGAGGGCTG3', reverse, 5'CATTTACCGAGAGGATCTTATCACCC3';
circRNA_014302	Forward, 5' TGGAGAGCTCGAATTCCAGAAC3', reverse, 5' AAAACAAGAGAGCCACCAGAGC3';
circRNA_001535	Forward, 5' AGCTACGGTGTCCTGAAACCTG3', reverse, 5' TTTCACAACGCTGACCACTGAC3';
circRNA_005522	Forward, 5' GCACCAAAGGCGATGGAGAAG3', reverse, 5'GTTGCTCTCTGAAGACCATCTGG3';
circRNA_013422	Forward, 5' ATGTTGGTGGATCCTGTTCGC3', reverse, 5' GGGTAGACCAAGACTTGTGAGG3';
ACTB	Forward, 5' GTACCACCATGTACCCAGGC3', reverse, 5' AACGCAGCTCAGTAACAGTCC3'.

chance. The P-value produced by topGO denotes the significance of GO term enrichment in the differentially expressed genes. The lower the P-value, the more significant the GO term (P ≤ 0.05 is recommended). Pathway analysis is a functional analysis mapping genes to KEGG pathways (https://www.kegg.jp/). The P-value (EASE score, Fisher's P-value or hypergeometric P-value) denotes the significance of the pathway correlated with the conditions. The lower the P-value is, the more significant the pathway.[16] The recommended P-value cutoff is 0.05.

Statistical Analysis

Data are presented as the mean ± SEM, the replication was performed for at least three times. Student's unpaired *t*-test was used for statistical analysis, as appropriate. All statistical analyses were performed using GraphPad Prism (version 9.5.1). A two-tailed P-value less than 0.05 was considered statistically significant.

Results

Basic Characteristics and Cardiac Function of the Animal Model

The mice in the normal control (NC) group were of normal size and had a good mental state. Compared with the NC group, the mice in the DCM group (n = 8) were fatter and more depressed and had slower reactions. At 21 weeks of age, the average weight was 42.00 g in the DCM group and 23.1 g in the NC group. The average ratio of heart weight/tibia length was 0.0095 in the DCM group, which was higher than that in the control group (P < 0.001). The fasting blood glucose level of the DCM group ranged from 16.7 mmol/l to 24.7 mmol/l, with a mean of 21.7 mmol/l (Figure 2A). Compared with the NC group, the DCM group had markedly increased fasting insulin (P < 0.001).

Compared with the NC group, the DCM group had increased LVIDd and LVIDs (Figure 3A and B) and decreased FS and EF. The mean ratio of E/A was 1.673 in the NC group and 2.573 in the DCM group (>2). Compared with the NC group, the DCM group had lower e′ value. Moreover, the DCM group had higher E/e' ratio compared with the NC group (Figure 3B), these indicated diastolic dysfunction in DCM group.

Pathological Analysis and Ultrastructure of Mouse Myocardial Tissue

Cardiac tissues were stained with H & E and Masson's trichrome. H & E staining showed that the DCM group had increased centrilobular necrosis, hydropic degeneration, and infiltration cell infiltration (Figure 2B). Masson's trichrome staining and transmission electron microscopy demonstrated that the DCM group had more extensive collagen deposition in the myocardial interstitium compared with the NC group (Figure 2C and D). The myocardium ultrastructure was displayed by electron microscopy. The results showed that the DCM group had large areas of cytoplasm without normal myofibrillary tissues, whereas the NC group had neatly arranged Z fibrils in myocardial cells (Figure 2D).

Different Expression of circRNAs

Compared with the NC group, the DCM group had 77 upregulated circRNAs and 135 downregulated circRNAs in the chromosomes (Figure 4A). Figure 4B shows a heatmap of circRNA distribution, while Figure 4C shows the circRNA volcano plots. The top 10 upregulated circRNAs and the top five downregulated circRNAs that were indexed by the circBase database are listed in Table 2. The top six upregulated circRNAs were mmu_circRNA_28667 (circPHF20L1), mmu_circRNA_32303 (circGDA), mmu_circRNA_20674 (circCLASP1), mmu_circRNA_25425 (circSYNJ2BP), mmu_circRNA_39272 (circNAA25), and mmu_circRNA_37101 (circMLLT3). Meanwhile, the top five downregulated circRNAs that were indexed by the circBase database were mmu_circRNA_014302 (circSLC8A1), mmu_circRNA_001535 (circPMS1), mmu_circRNA_005522 (circMKLN1), mmu_circRNA_013422 (circHIPK3) and mmu_circRNA_012617 (circMLIP). RT-qPCR was performed to validate circRNA expression. In db/db mice, the top four upregulated circRNAs were circPHF20L1, circGDA, circCLASP1, and circSYNJ2BP, and the top four downregulated circRNAs were circSLC8A1, circPMS1, circMKLN1, and circHIPK3 (Figure 4D). These results are in accordance with those of RNA microarray hybridization (Table 2).
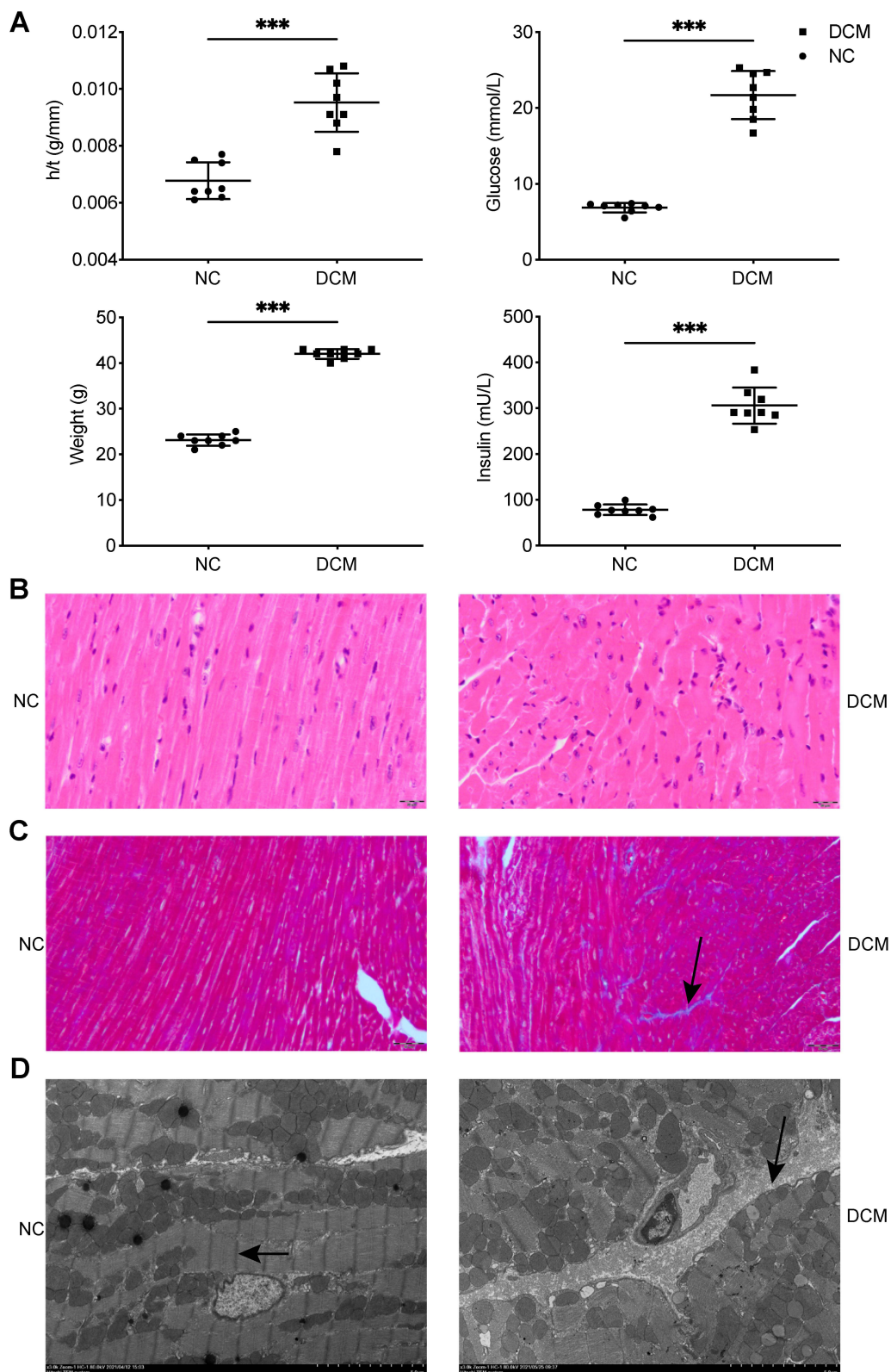
Figure 2 Establishment of db/db DCM mouse model. (**A**) Heart weight/tibia length ratio, body weight, and fasting blood glucose and insulin levels of the db/db and control mice (n = 8). (**B**) Cardiac tissue was stained with H & E (bar = 20 μm). (**C**) Masson's trichrome stain in cardiac tissue and collagen fraction (blue, arrow) (bar = 50 μm). (**D**) Myocardial tissue and mitochondria under electron microscopy (bar = 5.0 μm). Z fibrils (arrow in NC group), collagen deposition (arrow in DCM group). (**B**–**D**) n = 3, ***P < 0.001.
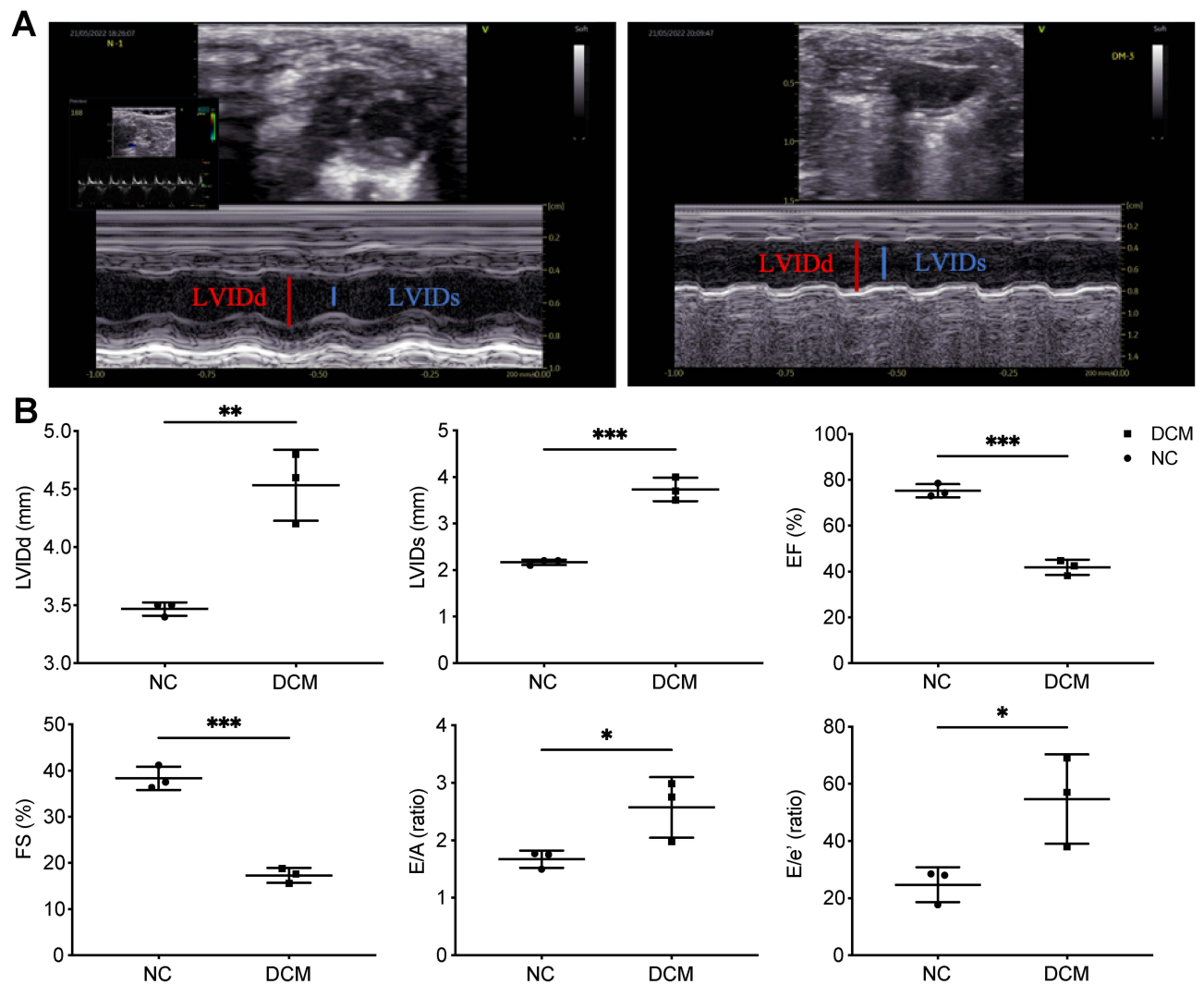**Abbreviations**: DCM, diabetic cardiomyopathy; H/T, heart weight/tibia length; NC, normal control.

Figure 3 Changes of cardiac structure and function in DCM mice. (**A**) Representative pictures of echocardiography. (**B**) Echocardiogram measurements (LVIDd, LVIDs, EF, FS, E/A, E/e') of the DCM and NC groups. n = 3, *$p < 0.05$, **$p < 0.01$, ***$p < 0.001$.
Abbreviations: LVIDd, left ventricular internal diastolic dimension; LVIDs, left ventricular internal diameter in systole; EF, ejection fraction; FS, fractional shortening; E/A: ratio of E wave to A wave; E/e': ratio of E wave to e' wave; DCM, diabetic cardiomyopathy; NC, normal control.

Compared with the NC group, the DCM group had remarkably increased expression levels of circPHF20L1 (fold change = 4.0263555, P < 0.05). CircPHF20L1, which is located on chromosome 15, is generated through the circularization of exons of PHD finger protein 20-like protein 1 (Phf20l1) and has a length of 466 nt.

CeRNA Network and Functional Analysis

A ceRNA network was constructed based on the differentially expressed circRNAs and bioinformatic prediction results to clarify the role of circRNAs in DCM mice (Figure 5). The top six upregulated circRNAs were circPHF20L1, circGDA, circCLASP1, circSYNJ2BP, circNAA25, and circMLLT3, whereas the top four downregulated circRNAs were circSLC8A1, circPMS1, circMKLN1, and circHIPK3, which were indexed by the circBase database. Some axes were related to fibrosis by ceRNA, including circPHF20L1/miR-29c-3p, miR-29b-3p, and miR-29a-3p/Col6a2; circCLASP1/miR-135a-5, miR-135b-5p, and miR-15a-5p/Mapk8; circCLASP1/miR-221-3p/Mapk13; circCLASP1/miR-182-5p, miR-15b-5p, and miR-15a-5p/Wnt7a; circCLASP1/miR-182-5p, miR-135a-5p, miR-135b-5p, miR-15b-5p, and miR-9-5p/Pik3r1; circNAA25/miR-6964-3p, miR-3620-5p, and miR-7682-3p/Samd9l; circSLC8A1/miR-29b-1-5p/Col12a1; and circMKLN/miR-135a-5p/Yes1; A detailed ceRNA summary was listed in Data S2.
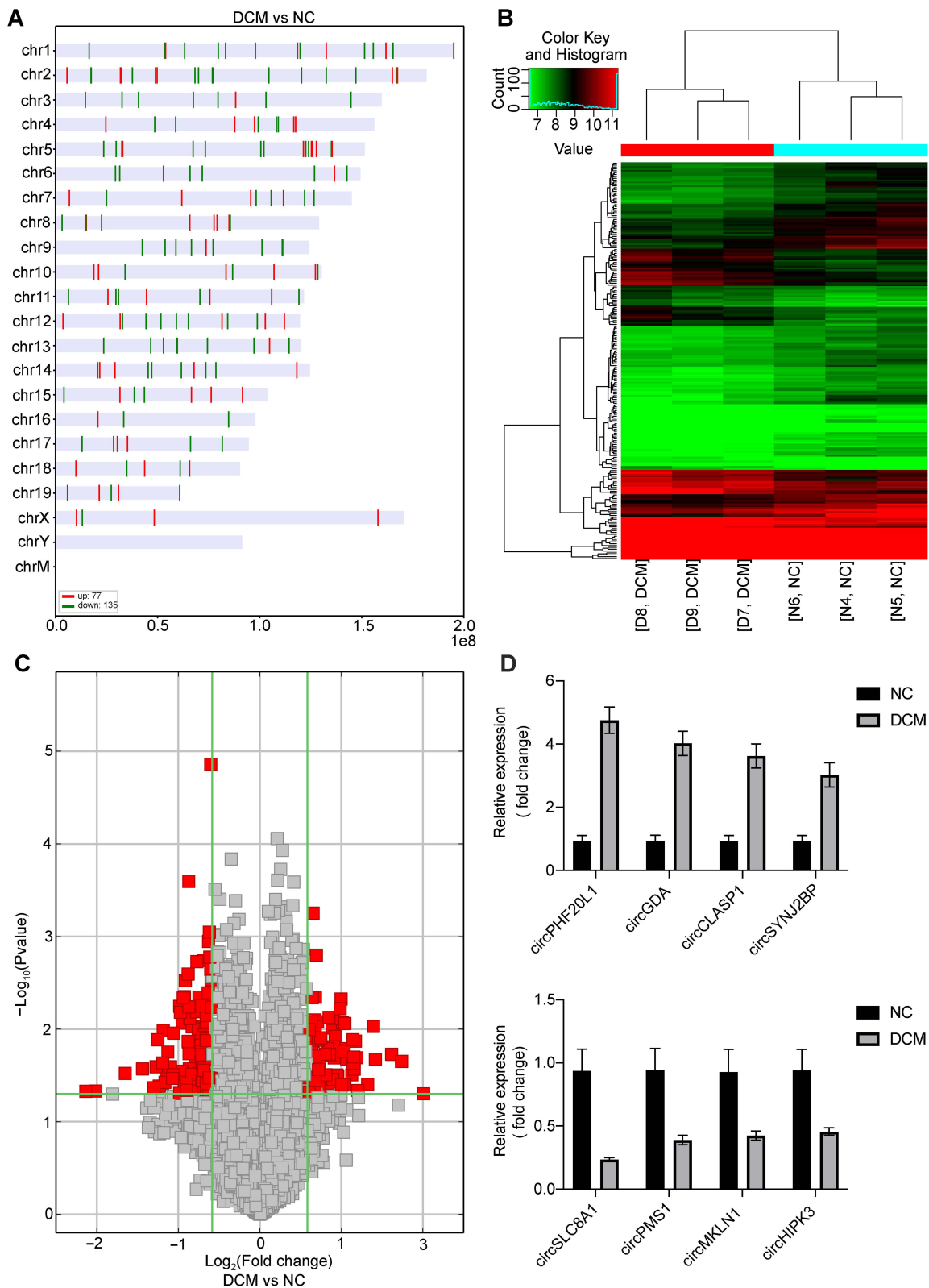
Figure 4 Overview of the detected circRNAs. (**A**) Distribution of differentially expressed circRNAs in chromosomes between the two groups. Upregulated (red) and downregulated circRNAs (green) in the DCM group vs NC group. (**B**) Hierarchical cluster analysis (heatmap) of differentially expressed circRNAs between the NC and DCM groups. (**C**) CircRNA volcano plots. The vertical lines correspond to 1.5-fold up and down, respectively, and the horizontal line represents a P-value of 0.05. The red point in the plot represents the differentially expressed circRNAs with statistical significance. (**D**) Some representative differentially expressed circRNAs were verified by RT-qPCR. n = 3; circRNA, circular RNA. circPHF20L1, mmu_circRNA_28667; circGDA, mmu_circRNA_32303; circCLASP1, mmu_circRNA_20674; circSYNJ2BP, mmu_circRNA_25425; circSLC8A1, mmu_circRNA_014302; circPMS1, mmu_circRNA_001535; circMKLN1, mmu_circRNA_005522; circHIPK3, mmu_circRNA_013422. **Abbreviations**: DCM, diabetic cardiomyopathy; NC, normal control.

Table 2 Differentially Expressed circRNAs in Myocardial Tissues Based on Fold Change

circRNA ID	P-value	FC (abs)	Regulation	GeneSymbol
mmu_circRNA_28667	0.049978294	4.0263555	Up	Phf20l1
mmu_circRNA_32303	0.022305223	3.3373264	Up	Gda
mmu_circRNA_20674	0.018721621	3.070012	Up	Clasp1
mmu_circRNA_25425	0.021272701	2.6734024	Up	Synj2bp
mmu_circRNA_39272	0.009375087	2.632007	Up	Naa25
mmu_circRNA_37101	0.039606401	2.4998485	Up	Mllt3
mmu_circRNA_39303	0.04601282	2.2993219	Up	Rad9b
mmu_circRNA_39417	0.020412384	2.2846202	Up	Aacs
mmu_circRNA_40979	0.013479433	2.2559389	Up	Atf7ip
mmu_circRNA_38420	0.027116693	2.2321756	Up	Depdc5
mmu_circRNA_014302	0.047061334	0.2275387	Down	Slc8a1
mmu_circRNA_001535	0.026882785	0.3689883	Down	Pms1
mmu_circRNA_005522	0.043059227	0.4062490	Down	Mkln1
mmu_circRNA_013422	0.046962145	0.4373786	Down	Hipk3
mmu_circRNA_012617	0.010386744	0.4398317	Down	Mlip

Notes: P-value calculated from unpaired *t*-test. FC (abs), the absolute ratio (no log scale) of normalized intensities between two conditions. Regulation, it depicts which group has greater or lower intensity values than the other group.

The parent genes of differential circRNAs were analyzed using KEGG and GO analyses to predict their biological functions. The top 10 pathways they were enriched in the DCM group were mainly related to biological processes, molecular functions and cellular components. The most enriched biological process was cellular process (Figure 5B). The pathway at the top of the list was the cellular process, because it had the smallest P-value and the largest number of genes enriched into the pathway, which represents all biological processes carried out at the cellular level. The definition of cellular process (GO:0009987): any process that is carried out at the cellular level, but not necessarily restricted to a single cell. For example, cell communication occurs among more than one cell, but occurs at the cellular level. In terms of molecular function, binding, protein binding, and ion binding were the most enriched (Figure 5C). Meanwhile, the most enriched cellular components were associated with cellular anatomical entity, intracellular, organelle, cytoplasm, and intracellular organelle (Figure 5D). In addition, KEGG pathway analysis showed the top 10 enriched pathways in the DCM group compared with the NC group (Figure 5E). Specifically, these differentially expressed circRNAs were mainly involved in the mitogen-activated protein kinase (MAPK) signaling pathway, which included 45 differentially expressed genes (eg, AKT3, KRAS, MAP2K4, MAPK10, MAPK13, MAPK8, MAPK8IP2, and TGFB3). KEGG pathway analysis also indicated that some other pathways, including the RAS signaling pathway, dilated cardiomyopathy, cardiac muscle contraction, hypertrophic cardiomyopathy, AMPK signaling pathway, and AGE-RAGE signaling pathway, were involved in diabetic complications. In addition, AKT, PIK, and WNT were differentially expressed genes that were involved in the development of cardiac fibrosis.

Discussion

In this study, the fasting blood glucose and insulin levels were considerably higher in db/db mice than in control mice. This finding suggests that db/db mice have T2DM characteristics. The type 2 diabetes mouse model is characterized by elevated blood glucose and insulin resistance. Although insulin levels are high, the physiological effects of insulin are diminished and do not effectively lower blood glucose, that is, insulin resistance, which is a characteristic of mice with type 2 diabetes.[17–19] DCM first manifests as diastolic dysfunction, which eventually progresses to cardiac hypertrophy and systolic dysfunction. The echocardiography results in the study suggested that db/db mice exhibited cardiac dysfunction. The high heart weight/tibia length ratio in db/db mice indicated that they had heart enlargement. Meanwhile, H & E staining suggested cell structural disturbance, and Masson's trichrome staining revealed more
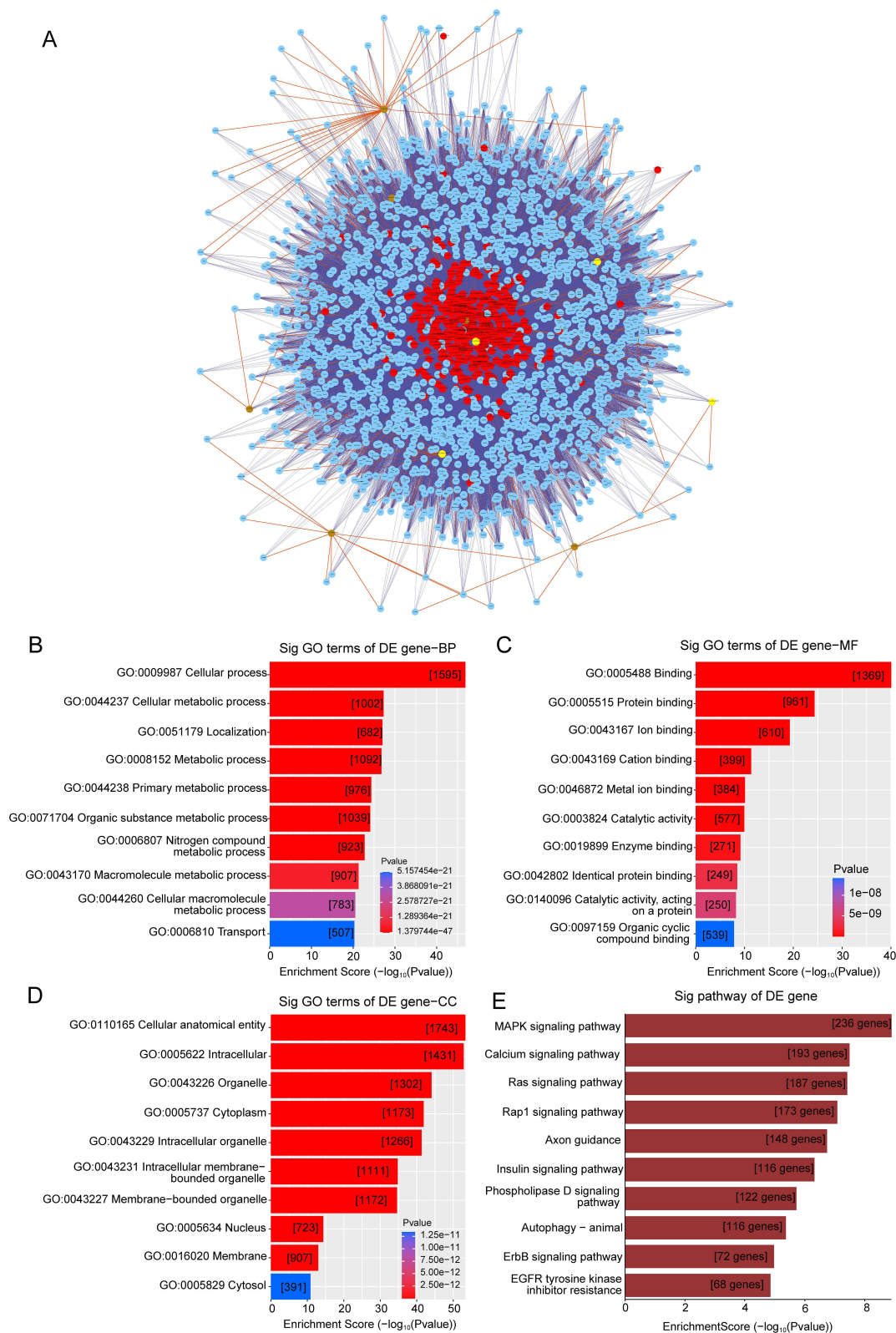
Figure 5 CeRNA network and functional analysis. (**A**) The ceRNA network was predicted by an online bioinformatics program. The top six upregulated circRNAs, and the top four downregulated circRNAs that were indexed by the circBase database, are shown. Nodes with red color are microRNAs, nodes with light-blue color are protein coding RNAs, nodes with brown color are up-circular RNAs, nodes with yellow color are down-circular RNAs. Edges with T-shape arrow represent directed relationships, edges without arrow represent undirected relationships (ceRNA relationship). (**B**–**E**) Differentially expressed circRNAs in the DCM group as indicated by GO and KEGG analyses.
Abbreviations: circRNA, circular RNA; DCM, diabetic cardiomyopathy; NC, normal control.

extensive collagen deposition in the DCM group, which was further confirmed by electron microscopy (Figure 2B–D). These results indicate that db/db mice had DCM fibrosis at the age of 21 weeks. A recent study found that db/db mice developed DCM fibrosis at the age of 20 weeks.[11]

In the present study, 212 circRNAs with significantly different expression were found within the two groups, which is much higher than the number reported in two recent studies.[9,20] The chromosomal distribution, composition, type, gene symbol, and length of these circRNAs were also analyzed. RT–qPCR verified the expression patterns from microarray hybridization, further confirming the accuracy of our microarray results. Among the upregulated circRNAs, circPHF20L1 was remarkably increased, which may have great research value. CircPHF20L1 is generated through the circularization of Phf20l1 exons and is 466 nt in length. Its length is between 200 bp and 3000 bp, which is convenient for later functional verification. PHF20L1 is a gene that was not previously involved in type 1 diabetes mellitus (T1DM), and its high expression is associated with lower diagnosis age in T1DM.[21] A previous study found that the expression of PHF20L1 was increased in tumor tissue sections of patients with ovarian cancer.[22] Based on the ceRNA regulatory network in Figure 5A, circPHF20L1/miR-29a-3p/Col6a2 may play a regulatory role in the development of myocardial fibrosis in DCM. The overexpression of circCLASP1, the third upregulated circRNA in the present study, greatly enhanced the stimulating effects of Huaier-induced immunogenic cell death.[23] A recent study showed that Wnt7a was also a fibrotic target gene.[24] Interestingly, circCLASP1 was upregulated in bd/db mice with cardiac fibrosis, and may regulate Wnt7a by inhibiting the activity of miR-182-5p. CircSlc8a1, the top downregulated circRNA in Table 2, was reported to be involved in cardiac hepatopathy. In a previous study, circSlc8a1 was decreased in mouse transverse aortic constriction hearts, and circSlc8a1 knockdown induced cardiac hepatopathy and fibrosis.[25] CircSLC8A1/miR-29b-1-5p/Col12a1 may be a novel axis in cardiac fibrosis. In our database, the expression of circSlc8a1 in the myocardium presented the same trend. However, some circRNAs exhibited inconsistent expression compared with those in previous studies. CircHIPK3 was downregulated in cardiac tissues from db/db mice. Yang et al found that the expression of circHIPK3 was elevated in a mouse T1DM model.[6] Another study found that circHIPK3 was upregulated in pulmonary fibrosis, and circHIPK3 silencing inhibited fibroblast-to-myofibroblast transition and suppressed fibroblast proliferation via the miR-338-3p/COL1A1, SOX4, or miR-30a-3p/FOXK axis.[26] Renal circHIPK3 was increased in folic acid-induced nephropathy, probably through miR-30a/TGFβ1.[27] The reason for the difference may be associated with the different models of diabetes and different organs. Other differentially expressed circRNAs listed in Table 2 have not been found in sequencing studies, which may be related to the different ages of mice collected from db/db samples.[5,9] The top 10 upregulated circRNAs and 3 downregulated circRNAs (circPMS1, circMKLN1, and circMLIP) found in the myocardium of db/db mice in the present study have not been reported to be involved in cardiomyopathy. CircPHF20L1, circGDA, circCLASP1, circSYNJ2BP, circNAA25, circMLLT3, mmu_circRNA_39303 (circRAD9B), mmu_circRNA_39417 (circAACS), mmu_circRNA_40979 (circATF7IP), mmu_circRNA_38420 (circDEPDC5), circPMS1, circMKLN1, and circMLIP appeared for the first time in the cardiomyopathy model, which may provide a target for subsequent treatment and a basis for subsequent research.

Among the differentially expressed circRNAs, some gene symbols from circRNAs (mmu_circRNA_38420 [DEPDC5] and mmu_circRNA_009939 [PEG3]) were associated with fibrosis. A study found that DEPDC5 down-regulation in immortalized hepatic stellate cells led to the increased expression of β-catenin and matrix metallopepti-dase 2.[28] In a rat carbon tetrachloride model, PEG3 was highly expressed in hepatic fibrosis tissues, and PEG3 downregulation led to a reduction in the histological changes of liver cirrhosis in vivo.[29] In another study, PEG3 silencing reduced ischemia/reperfusion-induced cardiac fibrosis in a mouse model.[30] In the circRNA-based ceRNA regulatory network, some miRNAs directly regulate cardiac fibrosis. Previous research has shown that miR-29b is remarkably downregulated in db/db mice.[31] A recent study demonstrated that miR-29b upregulation could inhibit cardiac fibrosis in CFs and in a mouse myocardial infarction model.[32] In the present study, the upregulated circRNA_41535 and circRNA_20422 in DCM mice have binding sites with miR-29b-2-5p. Thus, they may be novel targets in cardiac fibrosis. Zhang et al reported that miR-30a-5p was highly expressed in viral myocarditis mice with myocardial fibrosis.[33] It is worth exploring whether the circRNA_37409/miR-30a-5p/SOCS1 axis is a novel target axis in cardiac fibrosis. Previous research has shown that miR-203 is negatively linked to DCM fibrosis through PIK3CA via the PI3K/Akt signaling pathway.[34] Thus, whether circRNA_42260 and circRNA_004736 regulate cardiac

fibrosis and whether their mechanism is mediated by the circRNA_42260/miR-203/PIK3CA and circRNA_004736/miR-203/PIK3CA axes need to be investigated.

In addition, KEGG analysis showed that the differentially expressed circRNAs were mainly involved in the MAPK signaling pathway, which included 45 genes. Some of them were associated with cardiac fibrosis, including AKT3, KRAS, MAP2K4, MAPK10, MAPK13, MAPK8, MAPK8IP2, and TGFB3. The MAPK signaling pathway is closely related to cardiac fibrosis.[35,36] In the present study, the circCLASP1/miR-135a-5, miR-135b-5p, miR-15a-5p/Mapk8, and circCLASP1/miR-221-3p/Mapk13 axes may be novel targets in cardiac fibrosis. The Jun N-terminal kinase (JNK) pathway is an important pathway of the MAPK family. In our previous study, fasudil hydrochloride hydrate (a Rho-kinase [ROCK] inhibitor) could relieve the increase in JNK stimulated by HG in vitro[37] and in vivo,[38] suggesting that ROCK inhibition may be a novel therapeutic target for the prevention of diabetic cardiac fibrosis. Some studies have found that miR-29a-3p reduction promotes cardiac fibrosis in vivo.[39,40] Meanwhile, other studies have found that miR-29a-3p is involved in multiple organ fibrosis, including liver, lung, and renal interstitial fibrosis.[41–43] There are some binding sites among circPHF20L1, miR-29a-3p, and ROCK1 through miRDB (http://www.mirdb.org/). CircPHF20L1/miR-29a-3p/ROCK1 may play a regulatory role in the development of myocardial fibrosis in DCM.

Despite the findings, this study has some limitations. Only three mice were selected from each group for the myocardium circRNA microarray. The specific mechanisms of these circRNAs and more the results of bioinformatic analysis in myocardial fibrosis in DCM still need to be further investigated.

In conclusion, the present study revealed the differential expression of circRNAs in cardiac fibrosis in *db/db* mice. Functional enrichment analysis demonstrated the biological functions related to phenotype and the mechanism of cardiac fibrosis in DCM. The findings will provide some ideas for the prevention or clinical treatment of DCM at the molecular level through intervention with specific circRNAs.

Abbreviations
A, atrial contraction; AngII, Angiotensin II; a-SMA, α-Smooth muscle actin; ceRNA, Competitive endogenous RNA; CFs, cardiac fibroblasts; CircRNAs: Circular RNAs; circPHF20L1, mmu_circRNA_28667; circGDA, mmu_circRNA_32303; circCLASP1, mmu_circRNA_20674; circSYNJ2BP, mmu_circRNA_25425; circSLC8A1, mmu_circRNA_014302; circPMS1, mmu_circRNA_001535; circMKLN1, mmu_circRNA_005522; circHIPK3, mmu_circRNA_013422; DCM, Diabetic cardiomyopathy; E, early diastole; e', mitral annulus early diastolic velocity; E/A, ratio of E wave to A wave; E/e', ratio of E wave to e' wave; EF, ejection fraction; FS, fractional shortening; GO, Gene Ontology; H&E, hematoxylin–eosin; JNK, c. Jun N. terminal kinase; Phf20l1, PHD finger protein 20-like protein 1; LV, left ventricular; LVIDd, left ventricular internal diameter in diastole; LVIDs, left ventricular internal diameter in systole; KEGG, Kyoto Encyclopedia of Genes and Genomes; MAPK, Mitogen activated protein kinase; miRNAs, MicroRNAs; NC, Normal control; ROCK1, Rho-associated kinase 1; RT-PCR, Real-time polymerase chain reaction; T1DM, Type 1 diabetes mellitus.

Data Sharing Statement
CircRNA microarray data reported in this paper have been uploaded to NCBI and are publicly accessible at GSE239970.

Ethics Approval
This study was performed in line with the principles of the Declaration of Helsinki and the recommendations provided in the Guide for the Care and Use of Laboratory Animals by the National Institutes of Health. Approval was granted by the Animal Experimentation Ethics Committee of the Second Hospital of Hebei Medical University (NO. 2022-AE132).

Acknowledgments

Author Contributions

All authors made a significant contribution to the work reported, whether that is in the conception, study design, execution, acquisition of data, analysis and interpretation, or in all these areas; took part in drafting, revising or critically reviewing the article; gave final approval of the version to be published; have agreed on the journal to which the article has been submitted; and agree to be accountable for all aspects of the work.

Funding

Disclosure

The authors report no conflicts of interest in this work.

References

1. Kristensen L, Andersen M, Stagsted L, Ebbesen K, Hansen T, Kjems J. The biogenesis, biology and characterization of circular RNAs. *Nat Rep Genet*. 2019;20(11):675–691. doi:10.1038/s41576-019-0158-7
2. Jeck WR, Sorrentino JA, Wang K, et al. Circular RNAs are abundant, conserved, and associated with ALU repeats. *RNA*. 2013;19(2):141–157. doi:10.1261/rna.035667.112
3. Meng L, Lu Y, Wang X, et al. NPRC deletion attenuates cardiac fibrosis in diabetic mice by activating PKA/PKG and inhibiting TGF-β1/Smad pathways. *SCI ADV*. 2023;9(31):eadd4222. doi:10.1126/sciadv.add4222
4. Tang CM, Zhang M, Huang L, et al. CircRNA_000203 enhances the expression of fibrosis-associated genes by derepressing targets of miR-26b-5p, Col1a2 and CTGF, in cardiac fibroblasts. *Sci Rep*. 2017;7(1):40342. doi:10.1038/srep40342
5. Zhou B, Yu JW. A novel identified circular RNA, circRNA_010567, promotes myocardial fibrosis via suppressing miR-141 by targeting TGF-β1. *Biochem Biophys Res Commun*. 2017;487(4):769–775. doi:10.1016/j.bbrc.2017.04.044
6. Wang W, Zhang S, Xu L, et al. Involvement of circHIPK3 in the pathogenesis of diabetic cardiomyopathy in mice. *Diabetologia*. 2021;64(3):681–692. doi:10.1007/s00125-020-05353-8
7. Yuan Q, Sun Y, Yang F, et al. CircRNA DICAR as a novel endogenous regulator for diabetic cardiomyopathy and diabetic pyroptosis of cardiomyocytes. *Sigal Transduct Tar*. 2023;8(1):99. doi:10.1038/s41392-022-01306-2
8. Gu X, Jiang Y, Wang W, et al. Comprehensive circRNA expression profile and construction of circRNA-related ceRNA network in cardiac fibrosis. *Biomed Pharmacother*. 2020;125:109944. doi:10.1016/j.biopha.2020.109944
9. Dong S, Tu C, Ye X, et al. Expression profiling of circular RNAs and their potential role in early-stage diabetic cardiomyopathy. *Mol Med Rep*. 2020;22(3):1958–1968. doi:10.3892/mmr.2020.11248
10. Chen Y, Zhou J, Wei Z, et al. Identification of circular RNAs in cardiac hypertrophy and cardiac fibrosis. *Front Pharmacol*. 2022;13:940768. doi:10.3389/fphar.2022.940768
11. Pham T, Nguyen T, Yi J, et al. Evogliptin, a DPP-4 inhibitor, prevents diabetic cardiomyopathy by alleviating cardiac lipotoxicity in db/db mice. *Exp Mol Med*. 2023;55(4):767–778. doi:10.1038/s12276-023-00958-6
12. Tao H, Shi P, Zhao XD, Xuan HY, Gong WH, Ding XS. DNMT1 deregulation of SOCS3 axis drives cardiac fibroblast activation in diabetic cardiac fibrosis. *J Cell Physiol*. 2020;1:1.
13. Wang C, Liu W, Tan S, et al. Characterization of distinct circular RNA signatures in solid tumors. *Mol Cancer*. 2022;21(1):63. doi:10.1186/s12943-022-01546-4
14. Livak KJ, Schmittgen TD. Analysis of relative gene expression data using real-time quantitative PCR and the 2(-Delta Delta C(T)) Method. *Methods*. 2001;25(4):402–408. doi:10.1006/meth.2001.1262
15. Salmena L, Poliseno L, Tay Y, Kats L, Pandolfi P. A ceRNA hypothesis: the Rosetta Stone of a hidden RNA language? *Cell*. 2011;146(3):353–358. doi:10.1016/j.cell.2011.07.014
16. Lin J, Shi S, Chen Q, Pan Y, Alatas B. Differential Expression and bioinformatic analysis of the circRNA expression in migraine patients. *Biomed Res. Int*. 2020;2020:4710780. doi:10.1155/2020/4710780
17. Tan Y, Cao L, Jiao Y, et al. Inhibition of miR-543 alleviates cardiac fibroblast-to-myofibroblast transformation and collagen expression in insulin resistance via targeting PTEN. *Mol Cell Endocrinol*. 2023;576:111996. doi:10.1016/j.mce.2023.111996
18. Lu L, Ma J, Liu Y, et al. FSTL1-USP10-notch1 signaling axis protects against cardiac dysfunction through inhibition of myocardial fibrosis in diabetic mice. *Front Cell Dev Biol*. 2021;9:757068. doi:10.3389/fcell.2021.757068
19. Gómez-Banoy N, Guseh J, Li G, et al. Adipsin preserves beta cells in diabetic mice and associates with protection from type 2 diabetes in humans. *Nat Med*. 2019;25(11):1739–1747. doi:10.1038/s41591-019-0610-4
20. Wu X, Zhang S, Zhou X. Investigation on the differentially expressed circular RNAs in myocardium of mice with diabetic cardiomyopathy. *Zhonghua xin xue guan bing za zhi*. 2022;50(5):501–508. doi:10.3760/cma.j.cn112148-20220328-00216
21. Syreeni A, Sandholm N, Sidore C, et al. Genome-wide search for genes affecting the age at diagnosis of type 1 diabetes. *J Intern Med*. 2021;289(5):662–674. doi:10.1111/joim.13187
22. Alberto-Aguilar D, Hernández-Ramírez V, Osorio-Trujillo J, Gallardo-Rincón D, Toledo-Leyva A, Talamás-Rohana P. PHD finger protein 20-like protein 1 (PHF20L1) in ovarian cancer: from its overexpression in tissue to its upregulation by the ascites microenvironment. *Cancer Cell Int*. 2022;22(1):6. doi:10.1186/s12935-021-02425-6

23. Li C, Wang X, Chen T, et al. ViaHuaier induces immunogenic cell death circCLASP1/PKR/eIF2α signaling pathway in triple negative breast cancer. *Front Cell Dev Biol*. 2022;10:913824. doi:10.3389/fcell.2022.913824

24. Königshoff M, Eickelberg O. Listen to the WNT; It Talks: WNT7A drives epithelial-mesenchymal cross-talk within the fibrotic niche in idiopathic pulmonary fibrosis. *Am J Respir Cell Mol Biol*. 2023;68(3):239–240. doi:10.1165/rcmb.2022-0479ED

25. Wu N, Li F, Yang W, et al. Silencing mouse circular RNA circSlc8a1 by circular antisense cA-circSlc8a1 induces cardiac hepatopathy. *Mol Ther*. 2023;31(6):1688–1704. doi:10.1016/j.ymthe.2022.10.005

26. Zhang J, Lu J, Xie H, et al. circHIPK3 regulates lung fibroblast-to-myofibroblast transition by functioning as a competing endogenous RNA. *Cell Death Dis*. 2019;10(3):182. doi:10.1038/s41419-019-1430-7

27. Wu Y, Luan J, Jiao C, et al. circHIPK3 exacerbates folic acid-induced renal tubulointerstitial fibrosis by sponging miR-30a. *Front Physiol*. 2021;12:715567. doi:10.3389/fphys.2021.715567

28. Burza M, Motta B, Mancina R, et al. DEPDC5 variants increase fibrosis progression in Europeans with chronic hepatitis C virus infection. *Hepatology*. 2016;63(2):418–427. doi:10.1002/hep.28322

29. Zhu Y, Hu Y, Cheng X, Li Q, Niu Q. Elevated miR-129-5p attenuates hepatic fibrosis through the NF-κB signaling pathway via PEG3 in a carbon CCl rat model. *J Mol Histol*. 2021;52(3):491–501. doi:10.1007/s10735-020-09949-7

30. Cui L, Zhang Y, Ge X, et al. Downregulated PEG3 ameliorates cardiac fibrosis and myocardial injury in mice with ischemia/reperfusion through the NF-κB signaling pathway. *J Bioenerg Biomembr*. 2020;52(3):143–154. doi:10.1007/s10863-020-09831-x

31. Schellinger I, Wagenhäuser M, Chodisetti G, et al. MicroRNA miR-29b regulates diabetic aortic remodeling and stiffening. *Mol Ther Nucl Acids*. 2021;24:188–199. doi:10.1016/j.omtn.2021.02.021

32. Yuan J, Yang H, Liu C, et al. Microneedle patch loaded with exosomes containing MicroRNA-29b prevents cardiac fibrosis after myocardial infarction. *Adv Healthc Mter*. 2023;12(13):1.

33. Zhang Y, Cai S, Ding X, et al. MicroRNA-30a-5p silencing polarizes macrophages toward M2 phenotype to alleviate cardiac injury following viral myocarditis by targeting SOCS1. *Am J Physiol Heart Circ Physiol*. 2021;320(4):H1348–H1360. doi:10.1152/ajpheart.00431.2020

34. Yang X, Li X, Lin Q, Xu Q. Up-regulation of microRNA-203 inhibits myocardial fibrosis and oxidative stress in mice with diabetic cardiomyopathy through the inhibition of PI3K/Akt signaling pathway via PIK3CA. *Gene*. 2019;715:143995. doi:10.1016/j.gene.2019.143995

35. Zhao T, Kee H, Bai L, Kim M, Kee S, Jeong M. Selective HDAC8 Inhibition Attenuates Isoproterenol-Induced Cardiac Hypertrophy and Fibrosis via p38 MAPK Pathway. *Front Pharmacol*. 2021;12:677757. doi:10.3389/fphar.2021.677757

36. Wu M, Xing Q, Duan H, Qin G, Sang N. Suppression of NADPH oxidase 4 inhibits PM-induced cardiac fibrosis through ROS-P38 MAPK pathway. *Sci Total Environ*. 2022;837:155558. doi:10.1016/j.scitotenv.2022.155558

37. Zhou H, Zhang K, Li Y, Guo B, Wang M, Wang M. Fasudil hydrochloride hydrate, a Rho-kinase inhibitor, suppresses high glucose-induced proliferation and collagen synthesis in rat cardiac fibroblasts. *Clin Exp Pharmacol Physiol*. 2011;38(6):387–394. doi:10.1111/j.1440-1681.2011.05523.x

38. Zhou H, Li Y, Wang M, et al. Involvement of RhoA/ROCK in myocardial fibrosis in a rat model of type 2 diabetes. *Acta Pharmacol Sin*. 2011;32(8):999–1008. doi:10.1038/aps.2011.54

39. Hsu C, Liu I, Kuo H, et al. miR-29a-3p/THBS2 axis regulates PAH-induced cardiac fibrosis. *Int J Mol Sci*. 2021;22(19). doi:10.3390/ijms221910574

40. Wang R, Peng L, Lv D, et al. Leonurine attenuates myocardial fibrosis through upregulation of miR-29a-3p in mice post-myocardial infarction. *J Cardiovasc Pharmacol*. 2021;77(2):189–199. doi:10.1097/FJC.0000000000000957

41. Kong H, Song Q, Hu W, et al. MicroRNA-29a-3p prevents Schistosoma japonicum-induced liver fibrosis by targeting Roundabout homolog 1 in hepatic stellate cells. *Parasite Vector*. 2023;16(1):184. doi:10.1186/s13071-023-05791-4

42. Bu N, Gao Y, Zhao Y, et al. LncRNA H19 via miR-29a-3p is involved in lung inflammation and pulmonary fibrosis induced by neodymium oxide. *Ecotoxicol Environ Saf*. 2022;247:114173. doi:10.1016/j.ecoenv.2022.114173

43. Zhao M, Li N, Wan C, Zhang Q, Wang H, Jiang C. LncRNA CRNDE is involved in the pathogenesis of renal fibrosis by regulating renal epithelial cell mesenchymal-epithelial transition via targeting miR-29a-3p. *Mutat Res*. 2023;826:111817. doi:10.1016/j.mrfmmm.2023.111817